# A 0D Model for Rotating Detonation Engine Propulsive Performance Estimation

\* CNES

52, Rue Jacques Hillairet, 75612 PARIS Cedex
maitrelouan@gmail.com – bassam.gamal@cnes.fr

† Corresponding Author

#### **Abstract**

Rotating Detonation Engines (RDEs) are a promising and challenging alternative to classical rocket engine, offering the possibility to achieve sensitive improvements in propellant consumption through higher Specific Impulse (Isp) when compared to classical solution. Despite having focused the attention of many research activities through the last decades, this technology is still lacking a comprehensive set of analysis tools capable of covering the whole design process. Complex CFD approaches are usually needed in order to catch the physics behind RDEs operation, bringing complexity especially in the first steps of the design process, where fast and reliable iterations are preferred. In this paper, a simplified 0D model was developed to estimate the propulsive performances of an RDE along with its heating environment. The model is based on an idealized representation of detonation mechanisms, adjusted by the inclusion of non-idealities inherent to real prototypes. A pseudo 2D method based on the Method of Characteristics (MoC) is implemented to try giving a more accurate definition of the flow at the exit of the combustion chamber. A literature RDE can be simulated and the code has proven its ability to match experimental results by calibrating the real effects coefficients. Additionally, a thermal model was developed and found capable of reproducing both experimental and operational temperature time-evolutions.

#### 1. Introduction

In recent time, Pressure Gain Combustors (PGC) and their application to rocket propulsion have been a topic of increased interest among researchers. Traditional Liquid Rocket Engines (LRE), based on constant pressure combustion, have become extremely effective and optimized reaching very high efficiencies. Improving their performance is becoming more complex and expensive, and new breakthrough technologies seem to be needed in order to achieve substantial gains in space propulsion. In this frame, the use of detonation for propulsion was proposed back in the mid-XXth century by Zeldovich [1] and Voitsekhovshiï [2] but has been in the centre of a renewed attention since the beginning of the XXIst century. The higher thermodynamic efficiency of detonation in comparison with that of constant pressure combustion could theoretically lead to specific impulse gains as high as 10-15% with respect to LREs. In particular, Rotating Detonation Engines (RDEs) have concentrated a major research effort. They present several benefits over LREs such as an increased compactness at equal thrust, a lower injection pressure that would allow a significant simplification of the propellant feeding system or their good suitability for a combined use with an aerospike nozzle, in addition to their aforementioned increased thermodynamic efficiency. RDEs typically consist of an annular chamber in which one or several detonation waves propagate through continuously injected fresh reactants. Exceptionally high wave speed (over 1 km/s) often lead to a supersonic exhaust of the combustion products, which could therefore allow RDEs to run with a purely divergent nozzle. The physics and the structure of the flow inside an RDE remain challenging questions that are not completely well understood yet. The Technology Readiness Level (TRL) of RDEs still is quite low. The most advanced and powerful RDE prototype manufactured at the date, by NASA [3], is considered to have a TRL of 5. In 2021, JAXA performed the first RDE testing in space [4] and the Łukasiewicz Institute of Aviation in Warsaw flew the first rocket propelled by an RDE [5]. Annular-shaped RDEs have been widely tested in laboratories [6-9] mostly with gaseous propellants, and sometimes with a liquid-gaseous configuration [10] or even a liquid-liquid one [11]. Other chamber geometries showed encouraging features for RDE application and

specifically cylindrical (hollow) [12-14] and conical [5] combustors. The effect of exit conditions and nozzle integration onto the chamber was also investigated [15-16].

Although a hefty number of experiments and simulations was conducted on RDEs in the past decade, many phenomena inherent to their operation negatively affect propulsive performance and ward them off from ideal conditions. These were listed and are known [17-18] but their impact on performance and above all its quantification are poorly understood and are major obstacles to an optimized RDE design as well as to its scaling to an operational engine. The sizing of a new RDE always includes simulation steps prior to an expensive experimental campaign. However, highfidelity simulations such as 2 or 3-D CFD modelling are far too costly for the early-phases of the design, or when it comes to performing extensive parametric studies to investigate the influence of a more specific aspect on performance. A few low-order models were developed to meet these needs. Among them, Mizener and Lu [19] proposed an analytical, semi-empirical control-volume based approach in order to conduct parametric analyses and assess the effect of a range of design parameters on RDE performance. Walters et al. [20] derived a simplified ideal model from their experiment results in order to figure out which design parameters are of primary importance. Finally, Fievisohn and Yu [21] introduced an intermediate approach, based on the use of the Method of Characteristics (MoC). Unlike the aforementioned models, their method solves the internal flow in the chamber in two dimensions while remaining fast enough for optimisation loops. Even though these models offer already useful tools for quick RDE performance characterization, they may lack experimental or numerical validation besides being often adapted for theoretical parametric analyses or performance estimation of a single existing RDE. Moreover, they all consider ideal detonation conditions which is not consistent to predict the behaviour of a real engine. To the best knowledge of the authors, there is no available low-order model in the open literature that allows to perform simulations of RDE geometries in the frame of an early-phase project.

The purpose of this paper is to provide a pseudo 0-D model that can simulate and estimate the propulsive performances of an arbitrary RDE whether new or existing in the literature. The basis of the current work was a previous activity carried out at CNES which laid the foundations for a simplified RDE model. Some of the ideas presented in [21] are taken up. More precisely, a MoC calculation has been set up to partially solve the internal RDE flow. The developed tool, called DETOne, relies on the Cantera software for thermochemical calculations, and on the Shock and Detonation Toolbox by CalTech [22] for detonation calculation. It is designed as a "waterfall" structured code, consisting of a chain of functions executed sequentially until the final outputs are calculated. A wide range of parameters can be given as inputs including injector, chamber and nozzle geometry, propellant inlet conditions and numerical parameters of the simulation. The code outputs include propulsive performance, a simplified heat transfer analysis and a characterisation of the flow at various stages.

#### 2. Description of the model

#### 2.1 Simplified Model of the Internal Flow

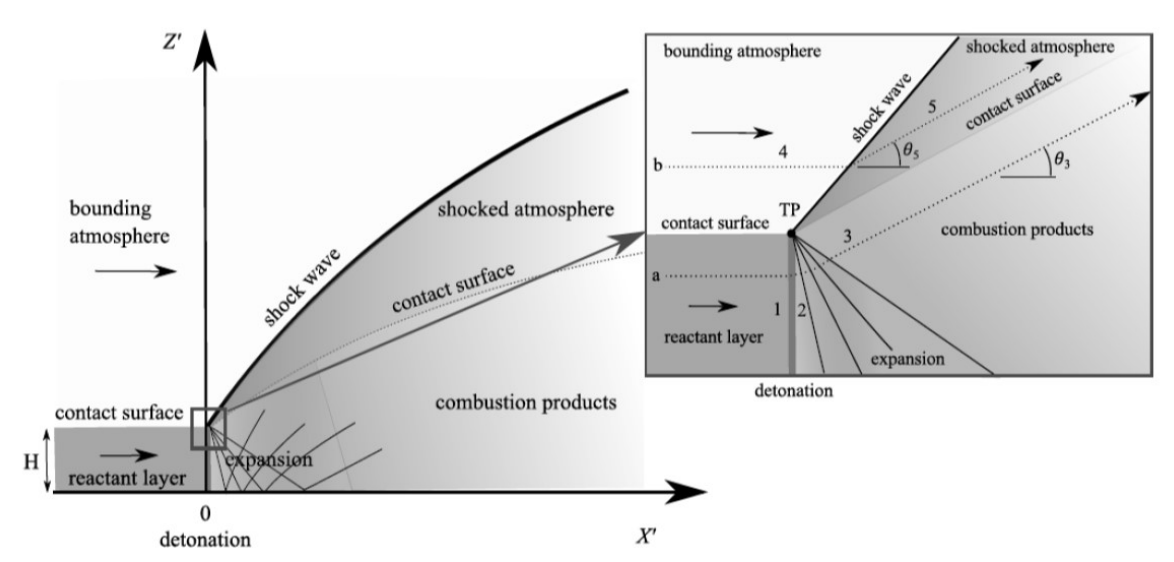


Figure 1: Simplified model for detonation of a uniform layer of thickness H and detail of triple point region (from [23])

The modelling of the internal flow around the detonation wave in the chamber is based on the approach proposed by Sheperd and Kasahara [23] and represented in Fig. 1. It can be considered as a canonical idealized view of an RDE flow. A reactant layer (1) is filled by freshly injected propellants which are burned through a detonation wave that produces an instantaneous pressure and temperature gradient (2). The combustion products are then expanded due to the difference in pressure between the chamber and the ambient atmosphere. A first expansion fan is generated at the top of the wave, through which the products expand to reach a third state (3). They continue expanding through the reflections of the initial fan, all the way until they reach the oblique shock wave attached to the detonation wave (4). They are finally shocked (5) and a slip line appears at the contact surface with the combustion products of the next cycle, when the detonation wave passes through the same location again. A mechanical equilibrium is assumed between states 1 and 4, as well as 3 and 5, such that their contact surfaces can be defined as slip lines. The oblique shock is considered as a straight line, while the shape of the slip line is discussed in a later section.

#### 2.2 Injection and Detonics

Initially, the fuel and the oxidizer are stored in separate plenums (state 0), at pressures  $P_f$  and  $P_{ox}$  and both at a temperature  $T_0$ . They are eventually assumed to be ideally premixed and injected (state 1) in the chamber at a pressure  $P_1$  given by:

$$P_{1} = C_{d_{P}} P_{0} \left( \frac{T_{0}}{T_{1}} \right)^{-\frac{\gamma}{\gamma - 1}} \tag{1}$$

Where  $C_{d_P}$  is a discharge coefficient (different for the fuel and the oxidizer),  $\gamma$  is the specific heat ratio of the mixture and  $P_0$  can be either  $P_f$  or  $P_{ox}$ . The injector is assumed to be choked, which is often the case in real engines due to important pressure gradients. Other quantities can thus be estimated at state 1 performing an isentropic expansion from state 0 and assuming ideal gas conditions. The choked assumption imposes the condition  $M_1 = 1$  on the Mach number, and the injection velocity can thus be defined as:

$$V_{inj} = \sqrt{\gamma r T_1} \tag{2}$$

With r being the specific gas constant of the mixture. Finally, the mass flow rate across an injection element can be derived using the Sutton relationship [24]:

$$\dot{m} = C_d A \sqrt{2\rho(P_0 - P_1)} \tag{3}$$

Where  $C_d$  is a discharge coefficient (common for both propellants),

The post detonation state (2) is derived using the well-known Chapman-Jouguet (CJ) model. It is an ideal representation of the detonation, considering the latter carried by a normal shockwave of infinitesimal thickness. Chemical reactions occur instantaneously both spatially and temporally. All detonation-related calculations are performed by the Shock and Detonation Toolbox (SDT) and for more detailed information, the interested reader will find additional insights in the related publication [22]. Nevertheless, real RDEs always show degraded conditions in comparison, with wave speeds ranging from 60% to 95% of the CJ velocity  $U_{CJ}$  for most experiments [7, 17]. This is a consequence of non-idealities mentioned earlier and as a result propulsive performances are altered. One should consider these effects and take them into account in the model in order to accurately simulate an RDE. The procedure used in this study is based on the models proposed by Chacon [25] and Barnouin et al. [26]. A "real effects" coefficient  $\omega$ , which physical definition is based on parasitic combustion representation, is introduced. Hence, only a molar fraction  $\omega$  of the fresh reactants is considered to be burned during the detonation. The remaining gases are considered to be consumed by a parasitic contact deflagration at the interface with the combustion products of the previous cycle (state 4). Both flows are then adiabatically mixed and detonated as displayed in Fig. 2.

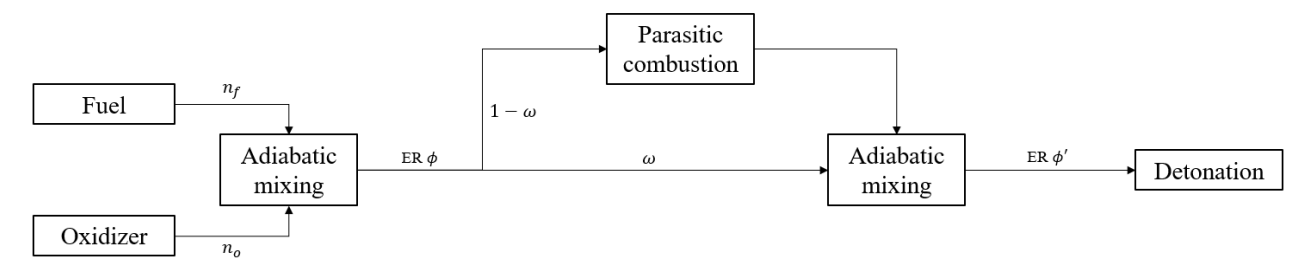


Figure 2: Schematic of non-idealities modelling

The Mach number at state 3, after the initial expansion fan, can be determined using the Prandtl-Meyer function  $\nu(M)$ . Sonic conditions, inherent to a CJ state, imply that  $\nu(M_2) = 0$ . It is thus straightforward that the flow deflection  $\delta$  will be given by  $\delta = \nu(M_3)$ . Accounting for mechanical equilibrium  $P_3 = P_5$ , and recalling that the flows at states 3 and 5 are assumed parallel, states 4 and 5 can be derived from state 3 for all angles in the range  $[0;\pi/2]$ . Flow deviation can be estimated by numerically assessing the intersection between the curves  $P_3(\delta)$  and  $P_5(\delta)$ . Hence, the correct Mach number at state 3 is calculated inverting equation (4):

$$\delta = \sqrt{\frac{\gamma + 1}{\gamma - 1}} \arctan \sqrt{\frac{\gamma + 1}{\gamma - 1}(M_3^2 - 1)} - \arctan \sqrt{M_3^2 - 1}$$
(4)

All other quantities at state 3 can be derived from state 2 using isentropic expansion relations. The derivation of state 4 is carried out likewise from state 3. Calculating state 5 requires a characterization of the attached oblique shock i.e. of its angle. It is most likely that the weak solution would naturally appear. Namely, the shock angle  $\sigma$  shall be comprised in the range  $[\mu_4; \sigma_{max}]$ , where  $\mu_4 = \arcsin\frac{1}{M_4}$  is the Mach angle, and  $\sigma_{max}$  is the limit angle, corresponding to  $M_5 = 1$ , that separates the strong and weak solutions and is defined as [21]:

$$\sin^2 \sigma_{max} = \frac{1}{4\gamma M_4^2} \left[ (\gamma + 1)M_4^2 - 4 + \sqrt{(\gamma + 1)[(\gamma + 1)M_4^2 + 8(\gamma - 1)M_4^2 + 16]} \right]$$
 (5)

It can finally be derived using the classic oblique shock relation, namely:

$$\frac{\tan(\sigma - \delta)}{\tan \sigma} = \frac{(\gamma - 1)M_4^2 \sin^2 \sigma + 2}{(\gamma + 1)M_4^2 \sin^2 \sigma} \tag{6}$$

All remaining quantities at state 5 are derived from state 4 by Rankine-Hugoniot equations.

### 2.3 Chamber flow modelling

In order to estimate the final performances of the engine as accurately as possible, it is necessary to assess the geometry of the flow in the combustion chamber. A major challenge is the derivation of the reactant layer height and of the injection length. Indeed, the extreme pressures existing immediately after the detonation wave may block the injection on a certain portion of the chamber perimeter  $(l_{bloc})$ . The determination of the remaining injection length  $l_{inj}$  is based on the two following relations:

$$t_{inj} = \frac{h_f}{V_{inj}} = \frac{l_{inj}}{D_w} \tag{7}$$

$$l_{bloc} + l_{ini} = \pi d_i \tag{8}$$

Equation (7) describes the characteristic injection time, with  $h_f$  being the reactant layer height (and thus the detonation wave height) and  $D_w$  the detonation wave speed. Equation (8) guarantees the coherence between the calculated lengths and the physical chamber perimeter,  $d_i$  being the internal chamber diameter. Several important assumptions are considered: the reaction layer is defined as a right triangle of basis  $l_{inj}$  and of height  $h_f$ , a single wave is present in the chamber and configurations with several detonation waves stay out of the scope of this study. Naturally, equations (7)

and (8) must be consistent with each other. However, a paradox exists. On the one hand, equation (7) shows that if the wave height is increased then, for a given injection velocity, the injection time increases too. On the other hand if  $h_f$  is increased, still at a given  $V_{inj}$ , then the injection length is decreased. And yet, considering equation (7), this would lead to a decrease of  $t_{inj}$ , which is inconsistent. Thus, a single equilibrium solution can exist to ensure a steady-state operation of the RDE. The detonation wave height can therefore be found by iterating on equations (7) and (8) from an initial guess.

More precisely, a MoC calculation is put in place to estimate the injection length, starting from the state 2 issued by the SDT and computing states 3 and 4. The other boundary condition for the MoC is the slip line between states 3/4 and 5. There is very little insight about the shape definition of the slip line, while it is crucial to define it in order to close the MoC problem. The decision made in this study was to adapt the Rao methodology for calculating minimum length diverging nozzles, based on the code developed by Dodson [27]. Although there is no direct physical bond between these two situations, the shape of the slip line is believed to be well approached in comparison with high-fidelity simulations, and it is considered by the authors as the best assumption currently available at the best of their knowledge to define the slip line in an RDE flow. The MoC put in place for determining  $h_f$  computes only the initial expansion fan and its first reflection, on the injection plate. It is called at every iteration, with a new value of the wave height. The calculation is deemed converged when the error between the computed injection length and the one derived from equation (8) are different by less than 0.01mm. Given that the typical order of magnitude for the detonation wave height of simulated RDEs in the literature is the 10 mm, the precision error would be no greater than 0.1%, which is far more than acceptable for a 0D code.

Once the wave height established, a new MoC calculation is performed in order to fully compute the flow at states 3 and 4, including characteristic reflections of the slip line. The intersection between the characteristic web and the oblique shock can then be determined, and all the section of the flow located afterwards is set at state 5. As mentioned earlier, state 5 is assumed uniform as the spatial variations of physical quantities at state 4 in the characteristic web are necessarily small in comparison of the important and instantaneous gradient imposed by the oblique shock. Fig. 3 presents an example of the flow definition inside the chamber as calculated by the tool developed in the present study.

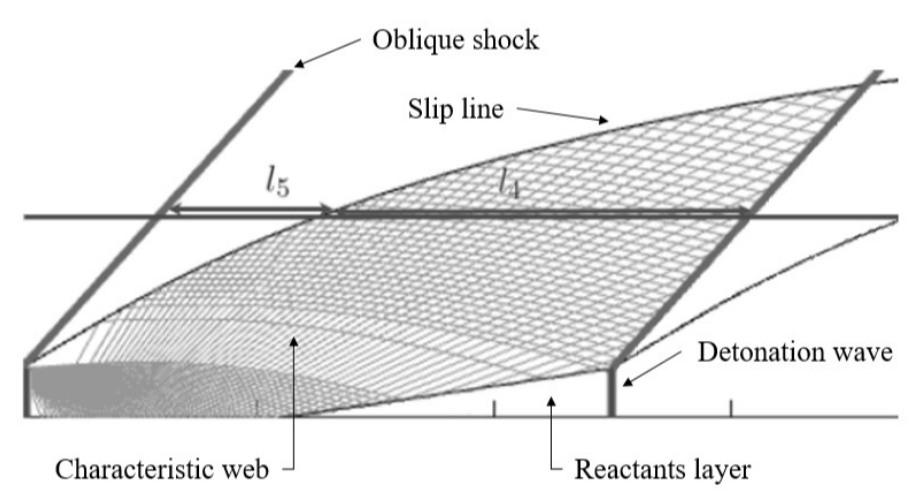


Figure 3: Representation of the internal RDE flow simulated during this study emphasizing on different flow features

#### 2.4 Propulsive performances

Having established an extensive definition of the internal chamber flow, it is possible to estimate the propulsive performances of the simulated RDE, and more precisely its overall thrust. The method presented in the precedent paragraph performs a general calculation, its domain being bounded by the slip line and the angle  $\delta$  of the initial expansion fan. However, it is imperative to define the height in the domain, that is to say the chamber length, at which the thrust will be evaluated. This length can therefore be directly set to simulate the exact geometry of an existing, or design phase RDE. As represented in Fig. 3 by the horizontal line, the chamber exit is divided in two portions. At first, a portion  $l_4$  is at state 4 and is comprised in the characteristic web which implies that a discretized spatial distribution of physic quantities is available. The remaining portion of the exit,  $l_5$ , is at uniform state 5. Adapting the technique described in [28], the thrust can be estimated through an integral calculation.

$$\rho \frac{D\mathbf{V}}{Dt} = -\nabla \cdot \left(P\bar{l} + \bar{\bar{\tau}}\right) + \mathbf{f}_b + \bar{\bar{f}} \tag{9}$$

From the momentum equation (9), neglecting viscous friction, volumetric forces and external forces, considering a control volume around the entire engine including the plenums (which implies an absence of inlet mass flow rate), one can derive the following general expression for the thrust:

$$F = \int [\rho U_y^2 + (P_e - P_{atm})] dA$$
 (10)

Where  $U_y$  stands for the outlet axial velocity,  $P_e$  and  $P_{atm}$  the exit and atmospheric pressures. Applying equation (10) to the domain represented in Fig. 3 ultimately leads to:

$$F = \frac{r_o^2 - r_i^2}{d_e} \left[ \int_{l_5}^{l_4 + l_5} \left[ \rho_4 U_{y4}^2 + (P_{e4} - P_{atm}) \right] dx + l_5 \left[ \rho_5 U_{y5}^2 + (P_{e5} - P_{atm}) \right] \right]$$
(11)

With  $r_o$  and  $r_i$  being the outer and inner radii of the annular RDE chamber. The code developed in this study requires a finite number of injection elements. As a consequence, the overall chamber mass flow rate can be evaluated multiplying the unit mass-flow rate of a single injection element by their total amount. This authorizes for an immediate calculation of the engine specific impulse. These calculations are only dealing with an isolated RDE chamber. However, the code was also designed to tackle complete engine, that is to say including a divergent, or a convergent-divergent nozzle. A simple near-1D model is implemented to perform such calculations. The flow at chamber exit is averaged for the sake of simplicity and injected into the Hugoniot equation:

$$\frac{dA}{A} = \frac{1 - M^2}{1 + \frac{\gamma - 1}{2} M^2} \frac{dM}{M} \tag{12}$$

Equation (12) is then integrated firstly on the convergent part of the nozzle, and finally on the divergent one. As the flow has been uniformed as it passed through the nozzle, the resulting expression of the thrust is much simpler and expressed as:

$$F = \bar{\rho}A_e \bar{U}_y^2 + (\bar{P}_e - P_{atm})A_e \tag{13}$$

#### 2.5 Thermal model

A major obstacle to RDE operation up until now is the extreme heat fluxes endured by the chamber inner walls. The incredibly high temperatures observed in RDEs and caused by the detonating nature of the combustion coupled with the supersonic velocities of the gases limit the vast majority of RDE prototypes to short burns (up to a few seconds) so far. This problem has been investigated by many [3-4, 10, 31-32], and some simplified models were proposed [12, 33] to analyze heat loads inside RDEs and give estimations of required cooling systems. This study does not seek to size such a cooling system, but to give an estimate of the highest temperature experienced by the RDE walls during operation. The purpose is to provide the user with the opportunity to assess the operating limits of an RDE for a given material. A 1D model has been set up to calculate the evolution of wall temperature. Several assumptions are made. The fluid temperature is kept constant and equal to the temperature of detonated gases  $T_2$ . Indeed, the highest heat fluxes were observed experimentally in the chamber bottom, and  $T_2$  is the highest temperature in the chamber which therefore gives the high bound for the calculation. Secondly, the wall is considered as semi-infinite, which implies that ambient conditions around the RDE are not considered. Furthermore, no distinction is made between the different walls in the chamber (flat injection plate, radial walls, etc.). The resulting temperature can be seen as the highest one possibly reached wherever in the RDE, which is sufficient to assess when material failure is likely to happen and thus setting the operation limit for a given RDE. Finally, the initial wall temperature is set to be equal to the propellants plenum temperature  $T_0$ .

The 1D heat equation without source term can be expressed as:

$$\frac{1}{\alpha} \frac{\partial T}{\partial t} = \frac{\partial^2 T}{\partial x^2} \tag{14}$$

Where  $\alpha$  is the thermal diffusivity of the considered wall material. In order to model the heat exchange between the hot detonated gases and the chamber wall, a Robin boundary condition is considered:

$$-k\left(\frac{\partial T}{\partial x}\right)_{x=0} = h(T_s(t) - T_2) \tag{15}$$

With k the thermal conductivity of the wall and  $T_s$  the wall temperature. Given the extreme temperatures induced by detonation (up to 3000-4000 K), the radiative heat transfer should be considered along with convection. A thermal equivalent circuit is set up accordingly. The convective resistor is defined as  $R_{conv} = \frac{D_h}{Nuk_g}$  where  $k_g$  is the fluidic conductivity,  $D_h$  the hydraulic diameter for an annular section and Nu the Nusselt number defined by the following correlation:

$$Nu = 0.023Re^{0.8}Pr^{0.4}f_{corr} (16)$$

With:

$$f_{corr} = \frac{0.75 \left(\frac{d_o}{d_i}\right)^{-0.17} + \left[0.9 - 0.15 \left(\frac{d_o}{d_i}\right)^{-0.6}\right]}{1 + \frac{d_i}{d_o}}$$
(17)

Besides, the radiative resistor is expressed considering a black body assumption (implying a unit emissivity  $\varepsilon = 1$ ) with the Stefan-Boltzmann law:

$$R_{rad} = \frac{1}{\sigma \varepsilon} (T_2^2 + T_s^2)(T_2 + T_s)$$
 (18)

With  $\sigma$  the Stefan-Boltzmann constant. Both resistors are set in parallel and the resulting total equivalent resistor is therefore  $R_{tot} = R_{conv}R_{rad}/(R_{conv} + R_{rad})$ . As a consequence, the overall heat transfer coefficient is defined as  $h = 1/R_{tot}$ . Finally, the solution of equation (14) under the boundary condition from equation (15) is given by:

$$\frac{T_s(x,t) - T_0}{T_2 - T_0} = 1 - \operatorname{erf}\left(\frac{x}{\sqrt{\alpha t}}\right) - \exp\left(\frac{hx}{k} + h^2 \frac{\alpha t}{k^2}\right) \left(1 - \operatorname{erf}\left(\frac{x}{\sqrt{\alpha t}}\right) + \frac{h\sqrt{\alpha t}}{k}\right)$$
(19)

## 3. Results and Discussion

# 3.1 Propulsive performance

The detonics module entirely relies on the SDT. This tool was already extensively validated against literature examples, experiments as well as the NASA CEA thermochemical code. Hence, it is deemed trustworthy and is not investigated nor validated further. In contrast, the calculation of the thrust along with the definition of the internal flow is compared in the present section with experimental results from the literature as well as with numerical simulations provided by ONERA.

A range of experiments, with an extensive description in the literature, is selected to serve as a reference. The works of Kawaski et al. [29] study the impact of varying the radius of the inner body of an annular nozzleless RDE on its performance and on the flow structure. Test 11 will be the reference case used from this publication. The studies of Bennewitz et al. [16,30] are unique in the sense that they collect the experimental results of campaigns conducted on a standardized RDE geometry in several American universities. One nozzleless case of each paper is considered, and the case from [16] with a convergent-nozzle of area ratio  $\varepsilon_c = 2.4$  is used to perform a validation of the full calculation using a nozzle.

Table 1: Reference cases simulated by DETOne and compared to experimental recordings

	ω	$D_{sim}$ [m/s]	$D_{exp}$ [m/s]
Kawasaki et al. [29]	0.9295	2331	1780
Bennewitz et al. [16]	0.9823	2442	1250
Bennewitz et al. [30]	0.9042	2383	1625

The employment of a real-effects coefficient, as well as of injection discharge coefficients, allows the code described in this paper to reproduce accurately the performances obtained during experimental measurements for a given RDE chamber geometry. Indeed, the coefficient  $\omega$  is used to adjust the code to the correct thrust, at a given mass-flow rate, which is obtained by adjusting the three discharge coefficients. For the three references mentioned in the previous paragraph, the obtained real effect coefficients are given in Tab. 1 (calculated for 30 characteristics). It is comforting to observe the need of such a coefficient in order to reproduce experimental results. Indeed, the CJ ideal model alone will always over-predict the performance as it doesn't account for numerous real effects wherein secondary (parasitic and commensal) combustions and waves, injection non-idealities or small-scale geometry effects. The present model can give some insight about the impact of such non-idealities but unfortunately, it is at the best of the authors knowledge impossible to quantify the separate impact of each phenomenon aforementioned, and  $\omega$  includes them all together, in spite of its definition relying exclusively on parasitic combustion. However, a well-adjusted  $\omega$  does not lead to a correct estimation of the detonation wave speed, as shown in Tab. 1. The underlying explanation is the nature of the real effects modelling provided by the code and will be more emphasized in a following paragraph. This error on the wave speed, although of high order, is not necessarily problematic as the influence of the wave speed on propulsive performance is believed to be secondary, although it is also considered than the thrust increases with the detonation speed. This effect is therefore compensated by the real effects coefficient, to a certain extent.

The first parameter that was studied is the number of characteristics used in the MoC. It is desirable to achieve efficient calculations, namely to reduce the computation time as much as possible. However, this should not be realized dropping results precision. Thus, a study of the impact of the number of characteristics is performed in order to determine a number suitable for further analysis while minimizing computation time. A first original guess is made at 30 characteristics. The real effects coefficient  $\omega$  is set at the corresponding value and kept constant as the number of characteristics is changed. The study is performed for calculations with the three references mentioned for a nozzleless RDE. Results are presented at Fig. 4 a). It is remarkable that the difference in the thrust calculated for a few thousand characteristics is only of 3% at most, for the case of [29] which has the lower thrust absolute value of all references. Moreover, it is clear that the calculation has converged above 1000 characteristics. It is therefore deemed acceptable to stay at 30 characteristics for subsequent developments. This is additionally advantageous when looking at the computation time. Indeed, the latter was found to be around 40 to 60 seconds at 30 characteristics while being four times greater at 1000 characteristics and almost 30 times higher at 5000 characteristics.

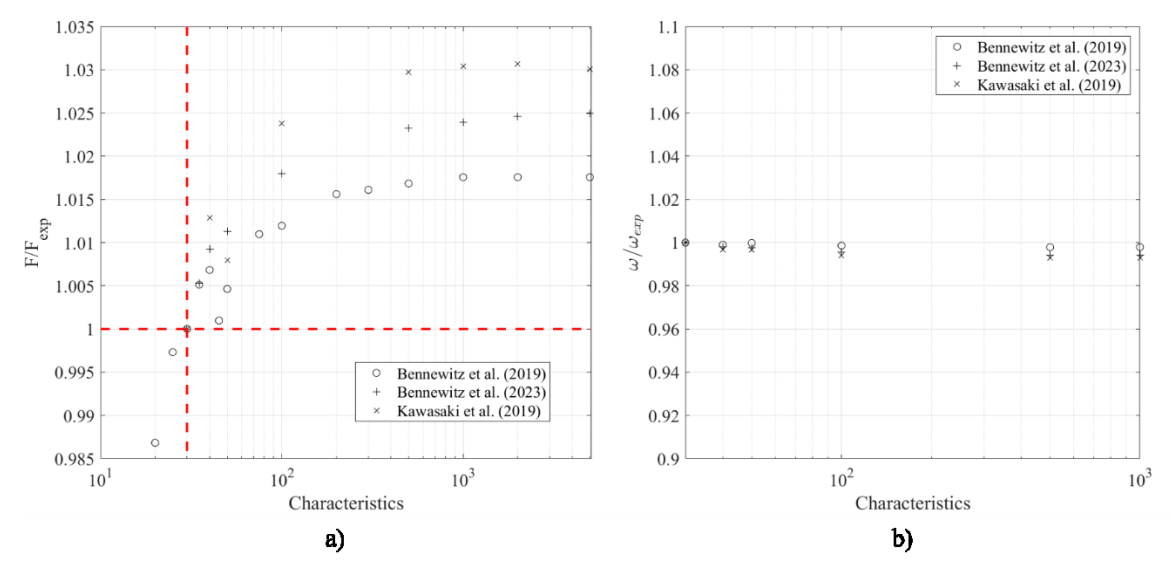


Figure 4: Thrust convergence a) and variation of  $\omega$  b) with the number of characteristics

It is also important to understand whether  $\omega$  is strongly influenced by the characteristics number or not. The same study as in the previous paragraph is performed, but allowing this time  $\omega$  to vary. It is recomputed for each number of characteristics such that no error is present in terms of thrust with the experimental reference case. Results are displayed on Fig. 4 b). A difference smaller than 1% is observed at most between low and high numbers of characteristics. Additionally, the values converge after a few hundred characteristics. The real effects coefficient is therefore believed to be fairly independent from the number of characteristics.

As discussed earlier in the present section,  $\omega$  as a matter of fact accounts not only for parasitic combustion, but also for many other non-idealities. One could have chosen to implement more real effects models in parallel in order to capture as much of them as possible, but this approach was considered risky, as no clear means of quantification of each effect exist so far. As said, DETOne is not capable of simulating RDEs with the correct thrust and wave speed at the same time. It is thus interesting to examine the effect of the real effects coefficients on the post-detonation state (2). The incomes of such a study are displayed in Fig. 5. The variation with  $\omega$  of the pressure and the temperature after the detonation wave as well as its speed were calculated varying the real effects coefficient and non-dimensionalizing them w.r.t. their CJ value (i.e. for  $\omega = 1$ ). The results obtained by the present model were also compared to the similar model of Chacon [25]. It can be seen that the influence of real effects is very unequal between different post-detonation quantities. For example, the pressure is far more decreased than the temperature and the wave speed. Indeed, the deflagration of 20% of the fresh reactants is sufficient to decrease the pressure to a third of its CJ value, while such a harsh alteration is never reached for the temperature. Additionally, reaching the experimental wave speeds in the code would require incredibly high rates of deflagrated gases, and in some cases couldn't even be reached. It is besides impossible to reach a feasible post-detonation state with the SDT for  $\omega < 0.2$ . Compared to the reference model of Chacon [25], the general behavior is conserved but slight and local divergences may appear. First, a difference in the slope and therefore in the magnitude of parameters is remarked. But it is also noticeable that for high enough  $\omega$ , the temperature can decrease faster (relatively) than the wave speed, contrary to what was modelled by Chacon. Such deviations could be explained by the different modelling of gas mixing after the deflagration (prior to the detonation), or to the second order by the difference in the detonation solver that was used (SDT in the present case versus NASA CEA in the reference).

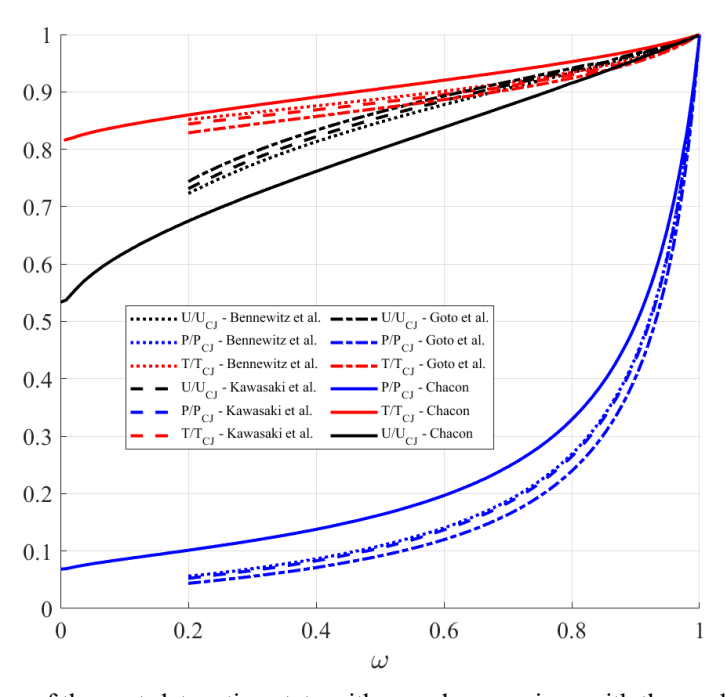


Figure 5: Evolution of the post-detonation state with  $\omega$  and comparison with the model of Chacon [25]

A complete RDE, including a convergent-divergent nozzle was then simulated. The purpose is to validate the nozzle module of the code and the changes it brings to performance assessment and more precisely thrust calculation. It is compared to the case of [16] with a nozzle of ratio  $\varepsilon_c = 2.4$ . The code still is capable of simulating the exact thrust, still at a slightly far wave speed. However, the variation of  $\omega$  is deemed to be important, with a value of almost 0.7, which corresponds to a 30% variation. The variation of the thrust with  $\omega$  was also investigated for this configuration, and the obtained results are presented in Fig. 6. It is clear by an analysis of the order of magnitude of the evolution of

the thrust with the real effects coefficient that it seems to be directly influenced by the post-detonation pressure, when comparing Fig. 5 and 6. A decrease greater than 80% is observed in terms of thrust for 30% of deflagrated gases, what shows the severe impact of parasitic combustion on propulsive performance.

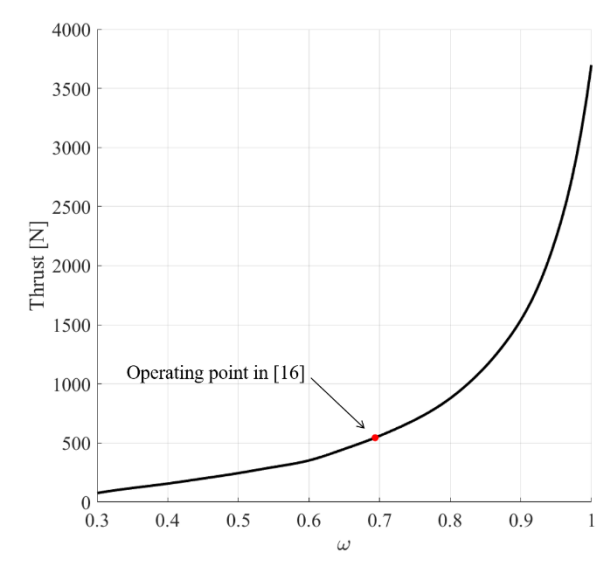


Fig. 6: Influence of  $\omega$  on the overall RDE thrust, reference case from [16]

# 3.2 Internal flow analysis

The characterization of the internal flow by DETOne is compared to a 2D CFD reference case provided by ONERA. A simulation of an unwrapped RDE combustion chamber was performed. The domain width (i.e. the chamber perimeter) is 0.5 m and its height (i.e. chamber length) is 0.2 m. The mass flow rate is 0.05 kg/s, the fuel is gaseous methane and the oxidizer gaseous oxygen. The injection is continuous over the entire chamber bottom and the propellants are ideally premixed. At the end of the chamber, a virtual nozzle is attached in order to ensure that all outlet gases are supersonic to avoid perturbations impacting the internal flow. It was shown that such a boundary condition does not affect the gas expansion inside the chamber itself. The same geometry was simulated in DETOne. A single injector is considered, and the area ratio between the chamber bottom and the injection area is conserved. The code inputs were set up to ensure that the same injection (state 1) conditions as in the CFD are met. The CFD doesn't account for real effects such as secondary combustion and the code is therefore ran with a unit  $\omega$  (all fresh reactants are detonated).

Table 2: Internal flow comparison between DETOne and the reference ONERA simulation

	DETOne	ONERA CFD
Detonation wave speed $D_w$ [m/s]	2356	2252
Detonation wave height $h_f$ [m]	0.0428	0.046
Shock angle $\beta$ [°]	38.5	$25^a$
Flow deflection $\theta_{max}$ [°]	57	$37^a$
Exit Mach number $M_e$	2.45	$1.66^{b}$
Exit axial velocity $U_{y,e}$ [m/S]	700	$1700^b$
Exit pressure $P_e$ [Pa]	1.377	$0.76^{b}$

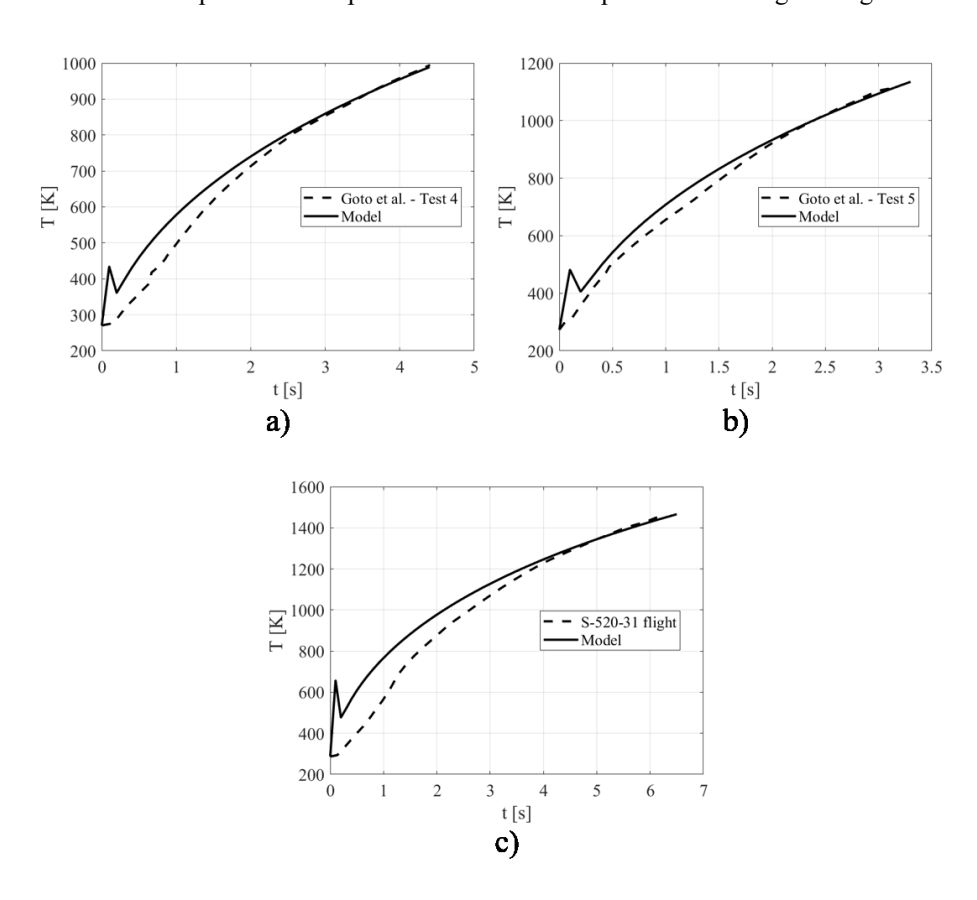
Exit temperature $T_e$ [K]	2413	$2837^{b}$
----------------------------	------	------------

<sup>&</sup>lt;sup>a</sup> Estimated near the triple point, relative to the y-axis

Tab. 2 illustrates the main flow quantities from the code alongside those from the reference high-fidelity simulation. First of all, the code's prediction of the detonation wave characteristics is near to that of the CFD, with an error around 5% for both the detonation wave speed and height, which is deemed acceptable for a 0D tool. On the contrary, flow angles and average exit conditions present an important deviation compared to the CFD, except for the exit temperature that remains of an acceptable order of magnitude. The code developed in this study does not aim to accurately simulate the internal structure of the flow inside an RDE chamber, remaining a 0D approach. However, the important divergence that can be noted implies that the real effect coefficient as well as discharge coefficients artificially correct the outputs of the code compensating for the error induced by the MoC approach. The methodology to estimate states 3 to 5 as well as flow angles described in section 2.3 potentially causes an intrinsic error, but it is doubted that more accurate results could be obtained by an analytical 0D approach. Moreover, the correct estimation of the detonation wave height confirms its relevance. On the other hand, it is believed that the most important source of error in DETOne could be the Rao-based description of the slip line. Indeed, this approach necessarily over-horizontalizes the flow, and this is amplified while the chamber becomes longer. In addition, the code assumes that the detonation wave is purely vertical, while an angle (approx. 8°) is observed in the reference CFD. Hence, a major challenge remains the definition of the slip line for a 0D code.

## 3.3 Thermal aspects

Two main references are used to validate the thermal model. The works of Goto et al. [34] investigated the heating environment on RDE experimental prototypes and provide a valuable source of detailed experimental temperature measurements. Two tests are considered as reference cases: tests 4 and 5. In addition, the flight data from [4] give a unique reference, allowing the model to be compared with real operating conditions. Both engines were manufactured in a C/C (carbon/carbon) composite which thermal properties are provided in the reference publications. Both papers furnish continuous thermocouple-based temperature measurements performed during the engines burns.



<sup>&</sup>lt;sup>b</sup> Averaged over the chamber exit

Figure 7: Comparison of the evolution of wall temperature between DETOne and the experimental data from [4] c) and [35] a) and b)

Fig. 7 presents the model defined in the present study in relation to the experimental data of the above-mentioned publications. It represents the evolution of wall temperature with time. From a behavioral perspective, the model satisfactory aligns with the experimental data. However, a slight deviation can be observed during the two first thirds of the simulation in all cases. Moreover, an overshoot peak is always present around t = 0.15s. This peak has no noticeable influence on further results, whereas it prevents from a use of the thermal model for extremely short simulations. Its origin remains undetermined but may be of a numerical nature. The magnitude of simulated temperature can be adjusted calibrating the real effects coefficient  $\omega$ . In the present cases, those values were set to 0.35 for [4] and 0.37 and 0.24 for [35] in tests 4 and 5 respectively. It is remarkable that these values stay close to each other, whereas they are really far from those needed to fit propulsive performance. A probable explanation is the assumption of  $T_2$  as a the fluidic temperature. This assumption certainly leads to an important overestimation of the wall temperature, especially compared to experimental cases for which the thermocouples were placed around 10mm up the injection plate. Nevertheless, the model itself is deemed valid for a 0D approach, keeping in mind that the amplitude prediction could be improved by enhancing the fluidic temperature estimation.

#### 4. Conclusions

The pseudo-0D model DETOne was developed and found capable of modeling existing RDE prototypes at a very low computational cost, in comparison with more advanced numerical simulations. Parasitic combustion as a way of degrading performance compared to an ideal CJ state detonation was successfully implemented based on previous works. However, there is potential for several refinements. The internal flow definition was found to be quite far from high fidelity simulations results and it is believed that a new methodology for slip line definition could seriously improve the restitution of the flow at RDE exit. Furthermore, a more accurate definition of the fluidic temperature in the thermal model would give a more realistic estimate of the wall temperature. The considered parasitic combustion non-ideality is proved to be a source of performance degradation, but it cannot explain deviations from experimental results alone. Other real-effect sources shall be studied, implemented and R&D activities shall be addressed in order to understand and master these physical phenomena with the goal of providing useful design tools to support future RDE developments. The results highlighted in this paper clearly show the need to better identify the set of non-idealities

#### References

- [1] I. B. Zeldovich. 1940. To the Question of Energy Use of Detonation Combustion". In: *Zhurnal Teknicheskoï Fiziki* tome 10, p. 542-568. doi: https://doi.org/10.2514/1.2
- [2] B. V. Voistsekhovskiï. 1960. Spinning Maintained Detonation. In: *Journal of Applied Mechanics and Technical Physics* tome 3, p. 157-164
- [3] T. Teasley et al. 2023. Current State of NASA Continuously Rotating Detonation Cycle Engine Development. In: *AIAA SCITECH Forum*. doi: <a href="https://doi.org/10.2514/6.2023-1873">https://doi.org/10.2514/6.2023-1873</a>
- [4] K. Goto et al. 2023. Space Flight Demonstration of Rotating Detonation Engine Using Sounding Rocket S-520-31. In: *Journal of Spacecraft and Rockets* 60.1, p. 273-285. doi: <a href="https://doi.org/10.2514/1.A35401">https://doi.org/10.2514/1.A35401</a>.
- [5] M. Kawalec et al. 2023. Development of a Liquid-Propellant Rocket Powered by a Rotating Detonation Engine. In: *Journal of Propulsion and Power* 39.4, p. 554-561. doi: https://doi.org/10.2514/1.B38771
- [6] S. Hansmetzger. 2018. Étude des modes de rotation continue d'une détonation dans une chambre annulaire de section constante ou croissante. PhD thesis, ENSMA, 2018.
- [7] S. M. Frolov, V. S. Aksenov, V. S. Ivanov et al. 2018. Rocket Engine with Continuous Detonation Combustion of the Natural Gas-Oxygen Propellant System. In: *Doklady Physical Chemistry* 478, p. 31-34. doi: https://doi.org/10.1134/S001250161802001X
- [8] B. R. Bigler et al. 2021. Rotating Detonation Rocket Engine Operability Under Varied Pressure Drop Injection. In: *Journal of Spacecraft and Rockets* 58.2, p. 316-325. doi: https://doi.org/10.2514/1.A34763
- [9] W. Armbruster et al. 2024. Experimental Investigation of a Small-Scale Oxygen-Hydrogen Rotating Detonation Combustor. In: *AIAA SCITECH Forum*. doi: https://doi.org/10.2514/6.2024-2612.
- [10] F. A. Bykovskiï and E. F. Vedernikov. 2009. Heat Fluxes to Combustor Walls during Continuous Spin Detonation of Fuel–Air Mixtures. In: *Fizika Goreniya i Vzryva* 45.1, p. 80-88. doi: https://doi.org/10.1007/s10573-009-0010-z
- [11] K. Ishihara et al. 2024. Nitrous Oxide/Ethanol Cylindrical Rotating Detonation Engine for Sounding Rocket Space Flight. In: *Journal of Spacecraft and Rockets*, p. 1-11. doi: 10.2514/1.A35824

- [12] K. Goto et al. 2021. Cylindrical Rotating Detonation Engine with Propellant Injection Cooling. In: *Journal of Propulsion and Power* 38.3, p. 410-420. doi: <a href="https://doi.org/10.2514/1.B38427">https://doi.org/10.2514/1.B38427</a>
- [13] R. Yokoo et al. 2020. Propulsion Performance of Cylindrical Rotating Detonation Engine. In: *AIAA Journal* 58.12, p. 5107-5115. doi: <a href="https://doi.org/10.2514/1.J058">https://doi.org/10.2514/1.J058</a>
- [14] R. Wiggins et al. 2023. Rotating Detonations in Hollow and Flow-Through Combustors. In: *AIAA Journal* 61.1, p. 86-96. doi: 10.2514/1.J061988
- [15] Z. Jiao et al. 2022. Experimental Study on the Performance of a Rotating Detonation Combustor with Different Outlet Restrictions. In: 13th International Conference on Mechanical and Aerospace Engineering (ICMAE). p. 233-238. doi: https://doi.org/10.1109/ICMAE56000.2022.9852903
- [16] J. W. Bennewitz et al. 2019. Performance of a Rotating Detonation Rocket Engine with Various Convergent Nozzles. In: *AIAA Propulsion and Energy Forum*. doi: 10.2514/6.2019-4299.
- [17] V. Raman, S. Prakash and M. Gamba. 2023. Nonidealities in Rotating Detonation Engines. In: *Annual Review of Fluid Mechanics* 55. p. 639-674. doi: https://doi.org/10.1146/annurev-fluid-120720-032612. org/content/journals/10.1146/annurev-fluid-120720-032612
- [18] B. Le Naour et al. 2023. Rotating detonation combustors for propulsion: Some fundamental, numerical and experimental aspects. In: *Frontiers in Aerospace Engineering* 2. doi: 10.3389/fpace.2023.1152429.2023.115242
- [19] A. R. Mizener and F. K. Lu. 2017. Low-Order Parametric Analysis of a Rotating Detonation Engine in Rocket Mode. In: *Journal of Propulsion and Power* 33.6, p. 1543-1554. doi:10.2514/1.B36432.
- [20] I. V. Walters et al. 2021. Performance Characterization of a Natural Gas—Air Rotating Detonation Engine. In: *Journal of Propulsion and Power* 37.2, p. 292-304. doi: https://doi.org/10.2514/1.B38087
- [21] R. T. Fievisohn and K. H. Yu. 2017. Steady-State Analysis of Rotating Detonation Engine Flowfields with the Method of Characteristics. In: *Journal of Propulsion and Power* 33:1, p. 89-99. doi: https://doi.org/10.2514/1.B36103
- [22] S. Kao et al. 2021. Numerical Tools for Shock and Detonation Wave Modeling. Tech. report Explosion Dynamics Laboratory, Graduate Aerospace Laboratories, California Institute of Technology.
- [23] J. E. Sheperd and J. Kasahara. 2017. Analytical Models for the Thrust of a Rotating Detonation Engine. Tech. report. California Institute of Technology
- [24] G. P. Sutton and O. Biblarz. 2001. Rocket Propulsion Elements. 7th Edition, John Wiley, Hoboken.
- [25] F. Chacon. 2020. Non-Ideal Phenomena in Rotating Detonation Combustors". PhD thesis, University of Michigan
- [26] P. Barnouin et al. 2023. Low-Order Model for Detonation Velocity Suppression in Rotating Detonation Combustors. In: *AIAA SCITECH Forum*. doi: 10.2514/6.2023-1291.
- [27] C. Dodson. 2014. Minimum Length Nozzle Design Tool. https://www.mathworks.com/matlabcentral/fileexchange/39499-minimum-length-nozzle-design-tool
- [28] A. R. Mizener and F. K. Lu. 2017. Low-Order Parametric Analysis of a Rotating Detonation Engine in Rocket Mode. In: *Journal of Propulsion and Power* 33.6, p. 1543-1554. doi:10.2514/1.B36432
- [29] A. Kawasaki et al. 2019. Critical condition of inner cylinder radius for sustaining rotating detonation waves in rotating detonation engine thruster. In: *Proceedings of the Combustion Institute* 37.3, p. 3461-3469. doi: https://doi.org/10.1016/j.proci.2018.07.070
- [30] J. W. Bennewitz et al. 2023. Experimental validation of rotating detonation for rocket propulsion. In: *Nature Sci Rep* 13. doi: <a href="https://doi.org/10.1038/s41598-023-40156-y">https://doi.org/10.1038/s41598-023-40156-y</a>
- [31] S. Randall et al. 2015. Numerical and Experimental Study of Heat Transfer in a Rotating Detonation Engine. In: 53rd Aerospace Sciences Meeting
- [32] S. J. Meyer et al. 2017. Experimental Characterization of Heat Transfer Coefficients in a Rotating Detonation Engine. In: 55th AIAA Aerospace Sciences Meeting. doi: 10.2514/6.2017-1285
- [33] Y. M. Kose and C. Murat. 2024. Regenerative Cooling Comparison of LOX/LCH<sub>4</sub> and LOX/LC<sub>3</sub>H<sub>8</sub> Rocket Engines Using the One-Dimensional Regenerative Cooling Modelling Tool ODREC *Applied Sciences* 14, no. 1:71. <a href="https://doi.org/10.3390/app1401007">https://doi.org/10.3390/app1401007</a>
- [34] K. Goto et al. 2019. Propulsive Performance and Heating Environment of Rotating Detonation Engine with Various Nozzles. In: *Journal of Propulsion and Power* 35.1, p. 213-223. doi:10.2514/1.B37196